ELSEVIER

Journal of Nuclear Materials 232 (1996) 166–180

journal of nuclear materials

A pragmatic approach to modelling thermal conductivity of irradiated UO_2 fuel: review and recommendations [1]

P.G. Lucuta [a,*], Hj. Matzke [b], I.J. Hastings [a]

[a] AECL, Chalk River Laboratories, Chalk River, Ont., Canada K0J 1J0

[b] Institute for Transuranium Elements, Joint Research Centre, European Commission, Postfach 2340, D-76125 Karlsruhe, Germany

Received 12 December 1995; accepted 28 May 1996

Abstract

The thermal conductivity of irradiated UO_2 fuel is discussed considering the effects of burnup (dissolved and precipitated solid fission products), porosity and fission-gas bubbles, deviation from stoichiometry and radiation damage based on single-effect results previously published on SIMFUEL (simulated extended burnup UO_2 fuel) and on radiation damage measurements. An analytical expression including factors describing the above effects is applied to the expression for unirradiated UO_2 thermal conductivity; it reflects the knowledge available today, and it is recommended for use with irradiated fuel. The expression is validated against available published data on thermal conductivity of irradiated fuel. This expression can be incorporated into fuel modelling codes to improve calculations of operating temperatures and predictions of behaviour of irradiated fuel under normal and accident conditions, including the extended burnup.

1. Introduction

The thermal conductivity of UO_2 has been investigated for over 35 years. It is one of the most important properties as it influences the fuel operating temperature, in turn affecting directly fuel performance and behaviour, particularly with respect to fission-gas release and swelling. There are several previous reviews [1–5] of UO_2 thermal conductivity, analyzing the experimental published data and the effects of different factors such as porosity and hyperstoichiometry. It is generally agreed that thermal conductivity of irradiated UO_2 is affected by the changes that take place in the fuel during irradiation: solid fission product build-up, both in solution and as precipitates, fission gas-bubble formation, possible deviation from stoichiometry and radiation damage.

There are only a few available published data on the thermal conductivity of irradiated UO_2 fuel [6–11]. Thermal conductivity of irradiated fuel has been determined indirectly from in-pile measurements of fuel central temperatures [6–9] or by direct measurements of thermal diffusivity on irradiated disc samples [10,11]. The data of Daniel and Cohen [6] published about 30 years ago, and analyzed by Marchandise [12], were considered the most reliable. The lack of published data is attributed to the difficulties involved in measurements, as well as to the proprietary nature of some of the more recent results. Despite the need for data on thermal conductivity of irradiated fuel, there are still difficulties in the interpretation of these results, because the effects from all the changes induced by irradiation are present, and overlap substantially, masking the effect of individual changes.

A useful way to quantify the changes in the fuel affecting thermal conductivity has been the use of SIMFUEL (simulated high burnup fuel) [13–15]. SIMFUEL replicates the composition and the microstructure (*without fission-gases and volatiles*) of irradiated fuel by introducing 11 stable additives into the UO_2, both those that are soluble in the fluorite-type lattice of the fuel and others that precipitate as second phases [13–15]. The composition of 3 and 6 at.% burnup SIMFUEL was provided in Ref. [14]. The thermal conductivity was determined for differ-

* Corresponding author.

[1] Presented at the 3rd IAEA Int. Coordination Meeting on Fuel Modelling at Extended Burnup, Bombay, India, Apr. 1–5, 1996.

0022-3115/96/$15.00 Copyright © 1996 Elsevier Science B.V. All rights reserved.
PII S0022-3115(96)00404-7

ent simulated burnups (1.5, 3, 6 and 8 at.% [2] burnup) from thermal diffusivity, specific heat and density measurements [16–21]. The use of SIMFUEL permitted the assessment and analysis of single effects on thermal conductivity: the effect of fission products [22–24] and the effect of deviation from stoichiometry [21] were quantified from the results in the form of factors applied to thermal conductivity of unirradiated UO_2.

Fission gases initially form in irradiated fuel as dispersed atoms within the lattice, and then coalescence into small intragranular bubbles [25]; they migrate, precipitate, re-dissolve and form larger inter-granular gas bubbles (especially in the high-temperature region of the fuel). The large bubbles then interlink into tunnels at the grain boundaries [26]. The solute gas atoms enhance the phonon scattering in the same way as the other dissolved fission products in the fluorite lattice. The dispersed and interlinked gas-bubbles also affect the fuel conductivity. Many models describe the effects of the fission-gas bubbles; it is outside our scope to review all these models. In particular, since the state of the fission-gas bubbles and their distribution in irradiated fuel is a function of burnup, linear rating and time–temperature history, the complex effects of these parameters are difficult to quantify.

Radiation damage creates additional defects in the fluorite lattice especially in the 'cold' regions of the fuel, at temperatures below 1100 K (at higher temperatures the defects from radiation damage are annealed as they form) [27]. Earlier work at Chalk River [27–29], based on in-reactor measurements of fuel central temperatures, determined the effect of radiation damage on fuel thermal conductivity. The effect of alpha decay-damage on thermal conductivity of plutonium and americium oxides has also been investigated for various temperatures and numbers of alpha disintegrations [30]. Currently, most fuel performance codes account for the effect of radiation damage on fuel thermal conductivity by using a constant cut-off value for thermal conductivity at temperatures below 800 K.

This paper provides an analytical expression for thermal conductivity of irradiated UO_2 fuel as a function of the temperature, (recommended for temperatures below 1900 K), that accounts for all the changes taking place during irradiation: solid fission-product build-up (dissolved and precipitated), pores and fission-gas-bubble formation, radiation damage and changes in the oxygen-to-uranium ratio (O/U). The model does not account for the effect of circumferential cracks on thermal conductivity, the greater porosity of the 'rim' region and of microbubbles.

2. Theoretical considerations

The thermal conductivity of UO_2 has two dominant contributions: conduction through lattice vibrations and conduction by electronic processes (conduction by radiation through the lattice can be neglected [3]). The former plays a major role for temperatures below 1900 K, and the latter is responsible for the observed increase in conductivity above 1900 K.

Currently, thermal-conductivity degradation is taken into account in fuel performance codes by additive resistivity terms for the burnup effect [16]. However, this formalism is the proper method only for 'weak' phonon scattering and can be only used to a certain burnup value [22]; the formalism adopted here is more general being valid over the whole range of burnup.

The expression for the parametric dependence of irradiated UO_2 thermal conductivity, λ, can be provided in a form of contributing factors for each individual effect:

$$\lambda = \kappa_1(\beta)\kappa_2(p)\kappa_3(x)\kappa_4(r)\lambda_0(T)\ (\mathrm{W/mK}), \qquad (1)$$

where $\kappa_1(\beta)$ is the burnup (β) dependence factor, $\kappa_2(p)$ is the porosity/bubbles (p) contribution, $\kappa_3(x)$ describes the effect of O/M ratio (x-deviation from stoichiometry), $\kappa_4(r)$ refers to the radiation damage and λ_0 is the analytical expression for thermal conductivity of unirradiated UO_2. Such an analytical expression can be easily adapted into fuel codes.

The effects of the changes taking place in irradiated UO_2 described by the four factors above, and their effects on thermal conductivity, are discussed and quantified in the following sections. The expression for each factor is derived from the available experimental data obtained by studying the 'single effect'. Finally, an analytical expression for the thermal conductivity of the irradiated UO_2 is derived and validated against published data by Daniel and Cohen [6], early Atomic Energy of Canada Limited (AECL) data [7], recent Belgonucleaire High Burnup Chemistry Club (HBC) data [8], and thermal diffusivity data obtained at JAERI [9] and Windscale [10] as part of the Halden program [11].

2.1. Thermal conductivity of unirradiated UO_2

To assess the thermal conductivity of irradiated UO_2 we briefly review the thermal conductivity of unirradiated UO_2 for which there are many measured published values. However, the experimental data are spread beyond the experimental errors of the measurements. This scatter of the data was discussed without a unanimous consensus on the reasons, among which were manufacturing differences, small deviation from stoichiometry or impurity effects [31].

The data from unirradiated UO_2 have been critically analyzed, summarized and reviewed in earlier papers [1–5]. It is generally accepted that the thermal conductivity is well described by two terms: a hyperbolic term for the lattice contribution through phonon-defect and phonon–phonon scattering processes and an exponential term for the polaron contributions (it becomes dominant for the high-temperature range $T > 1900$ K). The current knowl-

[2] 1 at.% ≈ 225 MW h/kg U ≈ 9375 MW d/te U.

edge leads to an analytical expression for the thermal conductivity of fresh fuel as a function of temperature (T) that includes four constants:

$$\lambda_0 = \frac{1}{A + BT} + \frac{C}{T^2}\exp\left(-\frac{D}{T}\right) \quad T \le T_0. \tag{2}$$

Changes of the exponential term of the polaron contributions were the main difference suggested in the various formulations. Harding and Martin [3] expressed thermal conductivity of fully dense UO_2 in the form

$$\lambda_0 = \frac{1}{0.0375 + 2.165 \times 10^{-4}T} + \frac{4.715 \times 10^9}{T^2} \exp\left(-\frac{16\,361}{T}\right) \text{ (W/m K)} \tag{3}$$

For fully dense (100% of theoretical density) UO_2, the analytical expression of thermal conductivity between 300 and 1900 K suggested by MATPRO [5] is slightly different with regard to the exponential term:

$$\lambda_0 = \frac{1}{0.04378 + 2.294 \times 10^{-4}T} + 1.429 \times 10^{-2} \exp \times (1.867 \times 10^{-3}T) \text{ (W/m K)}. \tag{4}$$

The Harding and Martin expression was used in a recent analysis [32] to fit earlier experimental measurements and constants were found to be only slightly different. Hyland [2] showed from the existing experimental values for the hyperbolic term, $1/(A + BT)$, the intrinsic parameter B should be in the range of 2.01 to 2.24×10^{-4} m W^{-1} and the extrinsic parameter is in the range of 2.466 to 5.746×10^{-2} m K W^{-1}. The values of these two parameters from various sources are listed in Table 1.

The thermal conductivity variation with temperature for unirradiated UO_2 given by Eqs. (3) and (4) are plotted in Fig. 1 along with two sets of experimental values that we have reported earlier [16,21]. The coefficients of the lattice contribution listed in the last column of Table 1 are from the best fit by Eq. (2) of the experimental data (dotted line). Our results are slightly higher than those fitted by Delette and Charles [32] using the expression recommended by Harding and Martin; nevertheless the constants of the lattice contribution term from our data and the Delette and Charles analysis are in very good agreement. MATPRO's fit of the experimental data is slightly lower; however, all the curves are in the band of known experimental uncertainties. Still, in our opinion, Harding and Martin's expression [3] gives a better representation of the thermal conductivity of unirradiated UO_2 and is used in our model for the conductivity of the unirradiated UO_2 fuel.

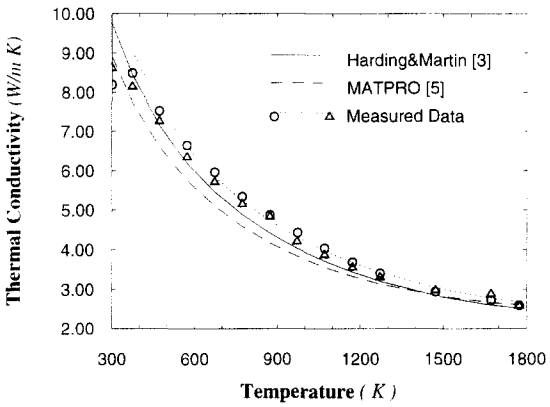

Fig. 1. Thermal conductivity of unirradiated fully dense UO_2 as a function of temperature according to two different analytical expressions. The band of different formulations reflects the scatter of the experimental data. The symbols represent two sets of earlier measurements [16,21].

2.2. Effect of solid fission-product build-up

The solid fission products formed during irradiation (dissolved and precipitated) affect the fuel thermal conductivity by changing the lattice contribution. Attempts have been made theoretically or experimentally to evaluate the effect of the fission products on thermal conductivity. Kleykamp [33] showed that the dissolved fission products lower the thermal conductivity, whereas the precipitated fission products increase the thermal conductivity. Experimental evidence of thermal conductivity degradation was obtained from one additive [34–36], or earlier work on simulated fuels [37,38]. However, the effects of the solid fission products on thermal conductivity were considered small and inadequately quantified [5].

Measurements of SIMFUEL thermal conductivity allowed the effects to be quantified as a function of the simulated burnup [16–19]. It was shown that a degradation in fuel conductivity occurs with the simulated burnup increase. Fig. 2 summarizes the results on thermal conductivity degradation (fully dense materials) for four different simulated burnups at temperatures between 300 and 1800 K. These results reflect the effect of the dissolved and precipitated fission products (*not* fission gases and volatiles) on fuel thermal conductivity. The experimental

Table 1
Values of the intrinsic and extrinsic parameters in the hyperbolic term of unirradiated UO_2 thermal conductivity from various sources

Source	MATPRO [5]	Washington [4]	Harding and Martin [3]	Lucuta et al. [22]
$B \times 10^{-4}$(m W^{-1})	2.29	2.25	2.165	2.202
$A \times 10^{-2}$(m K W^{-1})	4.378	3.50	3.75	3.53

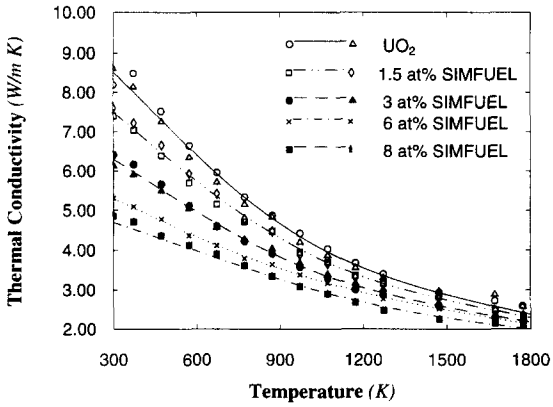

Fig. 2. Thermal conductivity of fully dense UO_2 and SIMFUEL with an equivalent burnup of 1.5, 3, 6 and 8 at.% as a function of temperature [16–19].

data in Fig. 2 were corrected to 100% theoretical density using a modified Loeb expression [16] that includes the temperature dependence.

The thermal conductivity experimental data from SIMFUEL were analyzed taking into account the effects of the precipitated and dissolved solid fission products in the UO_2 fluorite matrix (except for the fission gases). These two effects were previously quantified [22,23].

Thus the fission product factor, κ_1 consists of these two contributions:

$$\kappa_1(\beta) = \kappa_{1d}(\beta)\kappa_{1p}(\beta), \tag{5}$$

where κ_{1d} describes the effect of the dissolved fission products, and κ_{1p} accounts for the effect of the precipitates. A different approach in analyzing SIMFUEL data leads to an expression for thermal conductivity degradation in the form of additive terms to thermal resistivity [16,39].

2.2.1. The effect of dissolved fission products

The dissolved fission products lower the thermal conductivity and this degradation can be described by the phonon heat current theory [22,23]. The analysis of SIMFUEL results showed that the mass difference is the major factor to explain the experimentally observed degradation. This aspect of the analysis is discussed in detail elsewhere [24]. From the previous analysis [22], the reduction in fuel thermal conductivity caused by the solute fission products is described by the equation

$$\lambda_m = \lambda_0 \frac{\omega'}{\omega_D} \arctan\left(\frac{\omega_D}{\omega'}\right), \tag{6}$$

where ω'/ω_D was defined as a burnup dependent scattering parameter and λ_0 denotes the intrinsic thermal conductivity of the UO_2 (single crystal, defect free). However, in this analysis λ_0 is taken for unirradiated polycrystalline UO_2 fuel that always contains a number of defects. Introducing the burnup dependence for the scattering parameter in Eq. (6), the factor κ_{1d} that describes the effect of the solute fission products in the fluorite matrix is given by

$$\kappa_{1d}(\beta, T) = \left(n(\beta) + m(\beta)\sqrt{T}\right) \arctan\left(\frac{1}{n(\beta) + m(\beta)\sqrt{T}}\right), \tag{7}$$

where the parameters m and n contain the burnup dependence. Their expressions were derived from the SIMFUEL data and are given by the Eqs. (7a) and (7b):

$$m(\beta) = 0.0643/\sqrt{\beta}, \tag{7a}$$

$$n(\beta) = 1.09/\beta^{3.265}, \tag{7b}$$

where β is the burnup expressed in at.%. The fit of the SIMFUEL data [22,23] with Eqs. (7a) and (7b) is shown in Fig. 3.

Eq. (7) accounts for the effect of all solute fission products within the fluorite matrix, including fission-gas atoms and Pu build-up through the fission process. Note that for mixed oxide fuel (MOX) the effect of the Pu content and the related possibility of deviation from stoichiometry on thermal conductivity have to be taken into account from start-of-life and there are experimental data and correlations available, especially for the high Pu content of the fast breeder reactor fuel [40–42]. A unified treatment for the thermal conductivity of the unirradiated UO_2 and mixed oxide fuels ($U-PuO_2$; $UO_2-Gd_2O_3$) was also recently proposed [43].

2.2.2. The effect of precipitated fission products

The effective thermal conductivity of inhomogeneous media is a problem difficult to solve in general. The precipitated fission products (mainly metallic precipitates) are dispersed throughout the matrix as discrete, spherical particles with a diameter between 0.05 and 1 μm. Their conductivity is much higher than that of the matrix, and

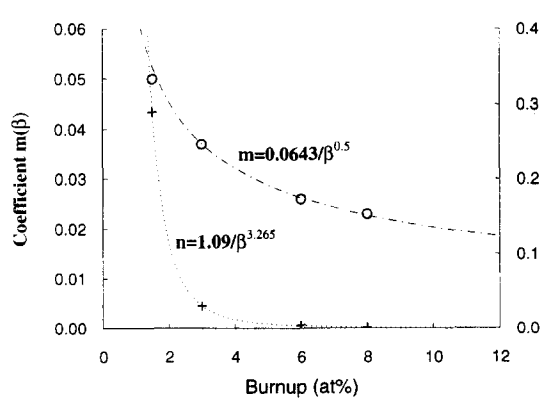

Fig. 3. The burnup dependence of the two constants from the expression of the dissolved fission-product factor fitting the earlier SIMFUEL data (note that in the limit as $\beta \to 0$ in Eq. (7), $\kappa_{1d} \to 1$).

they have therefore a positive contribution to the fuel thermal conductivity. The effect of the precipitated fission products was assessed theoretically [22,33], and their contribution to the thermal conductivity is depicted in Fig. 4 for the case of 8 at.% burnup SIMFUEL. However, additional experimental evidence on the effect of precipitated fission products on fuel conductivity obtained by measurements SIMFUEL with and without fission product precipitates could validate the theoretical approach.

The Maxwell factor κ_{1p} accounting for the contribution of precipitated fission products is

$$\kappa_{1p} = \frac{1+2q}{1-q} \approx \frac{1}{(1-q)^3}, \tag{8}$$

where q (<0.1) is the volume fraction of the precipitated phases (metals and $BaZrO_3$-type).

The maximum total volume fraction q is related to the burnup by $q = 0.0038\beta$ with the burnup β expressed in at.% [44]. Based on a perturbation treatment, Klemens analyzed a two-phase system with the conductivity as a function of the second phase position [45]. For high-conductivity inclusions non-homogeneously distributed, he suggested a correction factor:

$$\kappa_{1p} = \left(1 - \tfrac{5}{3}q\right)^{-1}. \tag{9}$$

Eq. (8) gives a higher value than Klemens' factor; however the difference is within a 4% margin, equivalent to experimental errors for burnups less than 10 at.% ($q <$ 0.038).

During irradiation, metallic fission products are formed everywhere across the fuel pellet. At the pellet periphery, in the cool region of the fuel, the metal precipitates are tiny (nanometer size), confined within the matrix and they contribute to the phonon scattering; thus their impact on

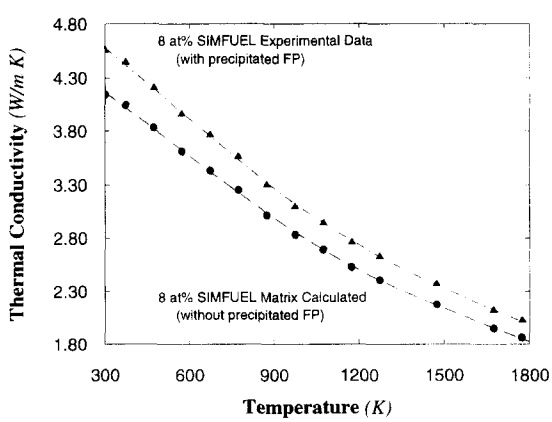

Fig. 4. Contribution of the precipitated fission products to fuel thermal conductivity is shown for 8 at.% burnup by the difference between the thermal conductivity of SIMFUEL and that calculated for the UO_2 fluorite matrix [22,23]. A 'Maxwell type' correction factor [22] was used to calculate the contribution of the precipitates to the fuel conductivity.

fuel conductivity is included in the dissolved fission product factor κ_{1d}. However, most of the metal fission products precipitate outside the fluorite matrix in the high temperature region (central part) of the pellet. This aspect can be taken into account by a transition function applied to the correction factor κ_{1p}. The distribution is temperature dependent and can be expressed by a transition function (symmetric sigmoid) with the transition height at 1200 K. Consequently, in irradiated fuel, the contribution from the precipitated fission products to the thermal conductivity, in the 600 to 1900 K temperature range can be expressed by a modified Maxwell type factor:

$$\kappa_{1p} = 1 + \frac{0.0114\beta}{1-0.0038\beta}\,\frac{1}{1+\exp(-(T-1200)/100)} \tag{10a}$$

or, by a modified Klemens' factor:

$$\kappa_{1p} = 1 + \frac{0.019\beta}{(3-0.019\beta)}\,\frac{1}{1+\exp(-(T-1200)/100)}, \tag{10b}$$

where β is the burnup in at.% and T the temperature in Kelvin. In this paper, the expression for the thermal conductivity of irradiated fuel will include the factor, κ_{1p}, given by Eq. (10b) to account for the precipitated fission products.

2.3. Effect of porosity and fission-gas-bubbles

The effective conductivity of a porous (sintering porosity plus fission-gas bubbles) fuel could be related analytically to the conductivity of the solid, λ_m and of the pores, λ_p. In UO_2 fuel, where $\lambda_p \lll \lambda_m$, the form of this relation is much simplified, as the heat transfer through the pores will take place by conduction through the fission gases or by radiation. The effect of porosity on UO_2 thermal conductivity has been extensively investigated and there are numerous analytical expressions suggested to calculate the porosity dependence. Rice [46], for instance, summarized 13 different theoretical relations that have been elaborated for various shapes of pores. A brief review of the porosity aspect for nuclear fuels can be found in the monograph on advanced fast breeder reactor fuels [47].

We distinguish between micro-bubbles formed within the lattice and large bubbles at the grain boundaries in the hot region of the fuel. The former are phonon scattering obstacles (their size is comparable with the phonon mean free path) and can be treated in the same manner as the tiny metallic precipitates and dislocation loops [48]; their effect on thermal conductivity is not directly proportional with the burnup and it is not considered in this paper; the latter constitute impediments to heat transfer and are considered in this section, using a treatment that also includes the initial porosity.

The *pore / bubbles factor*, $\kappa_2(p)$, is dependent on the volume fraction and the shape of the pores and bubbles. For small spherical pore/bubbles, uniformly dispersed, a modified Loeb expression [16], which includes the temperature dependence, can be used:

$$\kappa_{2p} = 1 - (2.58 - 0.58 \times 10^{-3} T) p, \tag{11a}$$

where p is the pore and bubble volume fraction of up to 9 vol.%. The Loeb expression is clearly inadequate for high porosities; it thus can not be generally used for irradiated fuel, despite the fact that is often applied for unirradiated UO_2.

The Maxwell–Eucken formula [44] includes a pore shape factor, and can be applied for a higher porosity amount (up to 20 vol.%):

$$\kappa_{2p} = \frac{1-p}{1+(\sigma-1)p}, \tag{11b}$$

where σ is a porosity shape factor, equal to 1.5 for spherical pores, larger for flatter pores and smaller for tubular porosities; many different measurements lead to different values for σ.

Nikolopoulos and Ondracek [49] used a general equation for a porous material:

$$\kappa_{2p} = (1-p)^{(1-\cos^2\alpha)/(1-F)+(\cos^2\alpha)/2F}, \tag{11c}$$

where F is a shape factor of the pores and $\cos^2\alpha$ is an orientation factor. They suggested 'a third-order bound' (an upper, $(1-p)^{1/2}$ and lower limit, $(1-p)^3$) for the effective conductivity λ_p/λ_m. The factors were defined for given assumptions (spherical, cylindrical pores).

Despite the fact that fuel codes include models on bubble morphology and size, the experimental data on their effect on fuel conductivity for higher porosities are scant in general. Pores and bubbles or segregated phases can be classified in two groups (according to the temperature perturbation around them). In the first group are the pores without any mutual interference: each pore is 'immersed' in the matrix far away from the others; and the influence of each pore can be estimated separately. The second group contains pores that exert a strong mutual interference; in this group the influence of a pore cannot be estimated without taking into account its neighbours. The sintering pores and intragranular fission-gas bubbles belong clearly to the first group if they are far from interlinkage (which is always the case under normal circumstances for intragranular pores in irradiated UO_2). On the other hand intergranular bubbles belong to the second group if they are close to interlinkage, or equivalently the porosity is progressively opening. Qualitatively, for the same amount of porosity, pores and bubbles from the first group will have less thermal resistance than the pore and bubbles of the second group. Along the pellet radius, the pore and bubble distribution and morphology is changing during irradiation and practically switches from the first group to the second as temperature and burnup increase. This points out that a simple formula for porosity is not sufficient to describe the thermal conductivity of the pores/bubbles in irradiated fuel.

The gas content of the pore and bubbles influences the thermal conductivity as well if conduction through the pores is assumed [50]. However, the conduction is significant only in well-defined situations with respect to the size, shape and gas content of the pores (which usually applies to small pores). Conduction is not dominant for large, unpressurized pores or when the radiation heat transfer becomes significant at high temperatures [50,51].

All these aspects have to be considered in a model that accounts for the effects of pores and bubbles on thermal conductivity of irradiated fuel. It is outside of the scope of this paper to develop a new model or adopt one of the many existing models on pore/bubbles in irradiated fuel. However, any model included in the fuel codes should include the initial porosity, the burnup, the linear power and power history as input data and ought to be validated against systematic experimental statistics on pore and bubbles population, size, morphology and distribution in irradiated UO_2 fuel. In this work, Eq. (11b) with the volume fraction p accounts for the pores and bubbles, realizing that this is a crude simplification of the real,complex situation described above.

2.4. Deviation from stoichiometry

Deviation from stoichiometry decreases the thermal conductivity of the fuel [52,53]. Recent results from SIMFUEL [20,21] showed that at high oxygen potentials (large deviation from stoichiometry) the effect of the fission-product accumulation is less significant, and the excess of oxygen plays the major role in the fuel conductivity reduction.

Analyzing the effect of deviation from stoichiometry on irradiated fuel conductivity there are two distinct regimes that would apply:

- normal operating conditions (NOC), and
- accident conditions and fuel defects.

2.4.1. Normal operating conditions

Excess of oxygen occurs in irradiated UO_2 from the fission process but can be buffered by fission products such as Mo and/or the cladding. Recent measurements of oxygen potentials in irradiated fuel [54,55] showed that for practical terms, the fuel is stoichiometric even at extended burnup when the 'rim' effect (subdivision of the UO_2 grains at burnups over 6.5 at.% [55]) is observed. Based on the available information, the factor $\kappa_3(x)$ to account for the effect of the deviation from stoichiometry on irradiated fuel thermal conductivity, *under normal operating conditions* is recommended as $\kappa_3(0) = 1$.

2.4.2. Fuel defects and accident conditions

The effect of deviation from stoichiometry on thermal conductivity is important for defected fuel and under accident conditions. In both cases the fuel becomes hyperstoichiometric and the thermal conductivity will decrease accordingly. The reduction in thermal conductivity observed experimentally in hyperstoichiometric UO_{2+x} and SIMFUEL [20,21] needs analysis based on the existing theoretical models in order to obtain an adequate analytical expression for the effect of deviation from stoichiometry. For SIMFUEL, at extended simulated burnups, samples simultaneously annealed at the same oxygen potential had practically the same thermal conductivity as the UO_{2+x} [20]. Based on an additive effect on thermal resistivity, $1/\lambda$ and the recent data from hyperstoichiometric UO_{2+x} and SIMFUEL the effect of the deviation from stoichiometry can be quantified. Fig. 5 shows the measured thermal conductivity of the UO_{2+x} and 8 at.% burnup SIMFUEL for various deviations from stoichiometry.

The 8 at.% SIMFUEL data were considered because they overlapped the results for UO_{2+x} at high oxygen potentials for temperatures above 900 K and do not have the change in slope observed in hyperstoichiometric UO_2 because of the precipitated U_4O_9 second phase [21].

The thermal resistivities, $1/\lambda_{2+x}$, of UO_{2+x} and SIMFUEL were fitted by the equation

$$\frac{1}{\lambda_{2+x}} = \frac{1}{\lambda_0} + \frac{1}{\lambda_x} = (a_0 + a_1 x) + (b_0 - b_1 x)T, \quad (12)$$

where the coefficients were determined from the experimental SIMFUEL data. The fit and the experimental values are shown in Fig. 6.

Consequently, the thermal conductivity of the oxidized fuel can be expressed by the equation

$$\lambda_{2+x} = \left(0.0257 + 3.336x + (2.206 - 6.85x)10^{-4}T\right)^{-1} \quad (13)$$

for deviations from stoichiometry up to 0.10. Our results

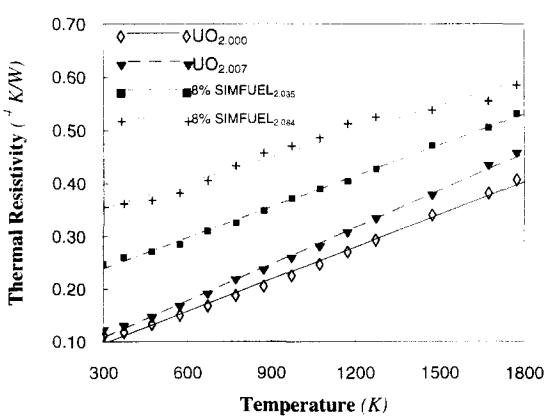

Fig. 5. The effect of deviation from stoichiometry in UO_{2+x} and SIMFUEL for the thermal resistivity plotted as a function of the temperature [21].

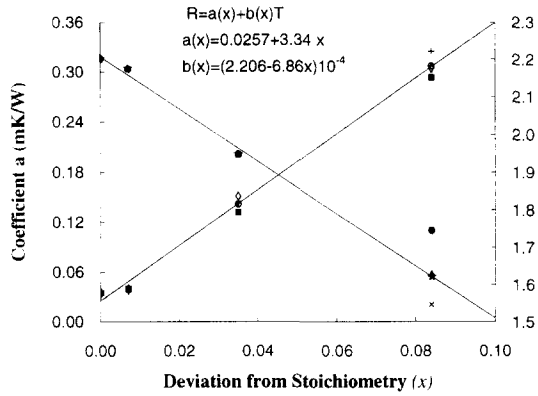

Fig. 6. The variation of the coefficients of the thermal resistivity expression with the deviation from stoichiometry.

are in reasonable agreement with the earlier results by Goldsmith and Douglas [52] in the range 670–1270 K. They obtained for UO_{2+x} a thermal resistivity varying linearly with x ($1/\lambda_{2+x} = 0.029 + 3.57x + 2.3 \times 10^{-4}T$), which matches well our expression. Eq. (13) will replace the intrinsic thermal conductivity of the UO_2 for defected fuel or accident conditions. Additional experimental data should be obtained for larger deviation from stoichiometry ($x > 0.1$) when higher oxides will form in defected fuel.

2.5. Radiation damage

Radiation damage from neutrons, α-decay and fission increases the number of lattice defects and consequently reduces the thermal conductivity of the fuel. Early work at Chalk River [27–29] showed that reactor radiation damage, for short irradiations, and below 1000 K, results in a maximum reduction of about 25% (see, however, the 60% below). The decrease was very rapid at the beginning of the irradiation (10^{19}–10^{21} n/m^2, hence order of minutes to hours) and no further effect was found above about 10^{23} n/m^2. A limiting value of 3.5 W/m K was reported for longer irradiations (up to 2.8×10^{24} n/m^2, corresponding to about a month of irradiation) [27].

Similar results were also obtained on irradiated ThO_2–1.3 wt% UO_2 [56] in out-of-pile measurements. Saturation was reached very early, i.e., in the range of 10^{20}–10^{21} n/m^2. Saturation was also reached very fast in a study of α-decay radiation in americium- and plutonium oxides [30]. The decrease in λ was up to 60%. Saturation in $\Delta\lambda$ occurs much faster than saturation in lattice parameter change, Δa, indicating that the defect concentrations affect λ and the lattice parameter, a, in a different way.

We see thus that the radiation-induced decrease in λ occurs early during irradiation. It is large at low temperatures, since the damage is stored in the lattice. Oxygen defects are known to anneal at around 500 K (hence below fuel operating temperatures), and uranium defects largely

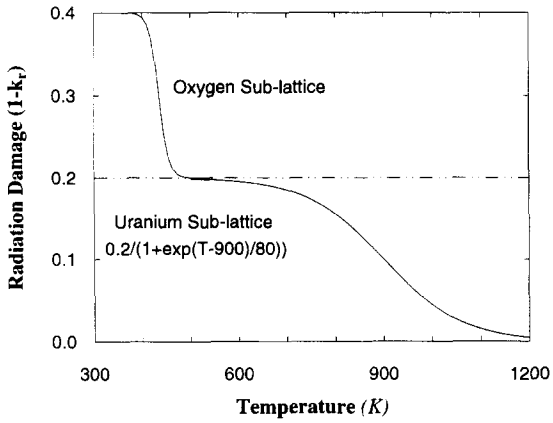

Fig. 7. The effect of radiation damage on UO_2 thermal conductivity as a function of the temperature.

anneal at higher temperatures, at around 1000 K. This explains why most changes are seen below 1000 K. Fig. 7 shows the relative reduction of UO_2 thermal conductivity caused by radiation damage: the first step is due to the oxygen defects and the second to the uranium defects. The distribution function for the second step (displayed in Fig. 7) is the analytical expression considered for the radiation damage effect.

However, even at higher temperatures, above 1000 K, a certain reduction in λ during irradiation is expected, because of the large Frenkel-defect production rate by the fission process. Since no results are available so far on this phenomenon, it is not included in the present treatment. Whereas fuel performance codes presently take radiation damage into account by a cut-off value for thermal conductivity at 800 K, we suggest the more physically sound picture given in Fig. 8 that takes into account the variation of the effect of radiation damage with the temperature. We do not suggest including fission dose (or fluence) as a

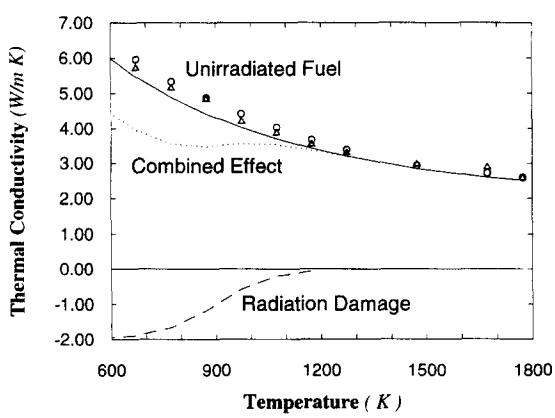

Fig. 8. Estimated effect of radiation damage on fuel thermal conductivity and the overlapped effect as a function of the temperature.

parameter since saturation is reached early in the fuel life. This treatment describes well the dominant effect, though at higher fluence, defect clusters, dislocation networks, etc., are formed and contribute to the radiation damage to a lesser extent.

3. Thermal conductivity of irradiated UO_2 – Summary and recommendation for algorithm

In summary, thermal conductivity of irradiated UO_2 fuel is affected by

- solid fission products- dissolved, and- precipitated;
- pores and fission-gas bubbles;
- deviation from stoichiometry;
- radiation damage;
- circumferential cracks.

In this paper, the effects from fission products, deviation from stoichiometry and radiation damage are well quantified and described as function of burnup and temperature (from room temperature to 1900 K). The uncertainties related to pore and fission-gas bubbles are also briefly discussed.

Based on the analytical expressions describing these effects, thermal conductivity of irradiated UO_2-fuel, for NOC up to 1900 K, can be expressed by

$$\lambda = \kappa_{1d}\kappa_{1p}\kappa_{2p}\kappa_{3x}\kappa_{4r}\lambda_0, \tag{14}$$

where

$$\lambda_0 = \frac{1}{0.0375 + 2.165 \times 10^{-4}T} + \frac{4.715 \times 10^9}{T^2} \exp\left(-\frac{16361}{T}\right) \tag{14a}$$

is Harding's expression for the thermal conductivity of unirradiated UO_2;

$$\kappa_{1d}(\beta) = \left(\frac{1.09}{\beta^{3.265}} + \frac{0.0643}{\sqrt{\beta}}\sqrt{T}\right) \arctan\left(\frac{1}{1.09/\beta^{3.265} + \left(0.0643/\sqrt{\beta}\right)\sqrt{T}}\right) \tag{14b}$$

quantifies the effect of the dissolved fission products;

$$\kappa_{1p} = 1 + \frac{0.019\beta}{(3 - 0.019\beta)} \frac{1}{1 + \exp(-(T - 1200)/100)} \tag{14c}$$

describes the effect of precipitated solid fission products;

$$\kappa_{2p} = \frac{1 - p}{1 + (\sigma - 1)p} \tag{14d}$$

is the modified Maxwell factor for the effect of the pore and fission-gas bubbles;

$$\kappa_{3x} = 1 \tag{14e}$$

shows *no* deviation from stoichiometry under NOC;

$$\kappa_{4r} = 1 - \frac{0.2}{1 + \exp((T - 900)/80)} \tag{14f}$$

characterizes the effect of radiation damage. In the above expressions: T represents the temperature in Kelvin, β is the burnup in at.%, p is the volume fraction of pores and bubbles, and σ is the pore shape factor (with a value of 1.5 for spherical bubbles in the absence of other data). Fig. 9 displays the predicted UO_2 thermal conductivity as a function of temperature for six different burnups between 0 and 10 at.%.

The reduction in thermal conductivity is significant especially in the low-temperature region of the fuel where radiation damage occurs. There is a large reduction predicted in the 600 to 700 K range at extended burnup. Note that above 7 at.% burnup the 'rim' structure forms in light water reactor (LWR) fuel [57,58], which — because of increased porosity — may give a further contribution to the thermal conductivity reduction. For the higher temperature region, above 1500 K, the model shows no significant reduction over 6 at.%, although the effect of the changes in pores and fission gas bubbles is not included.

For *defected fuel and / or accident conditions*, the expression for intrinsic conductivity λ_0 is replaced by Eq. (13) describing the effect of the deviation from stoichiometry based on the UO_{2+x} and hyperstoichiometric SIMFUEL data. However, a better understanding of the excess of oxygen effect is required to quantify the data in a factor form.

The effect of cracks formed in irradiated fuel and their effect on thermal conductivity was omitted. This aspect is important especially if circumferential cracks develop in the fuel pellet during irradiation and act as a gap for the heat transfer. Nevertheless, it appears that the circumferential cracks during cooling between the plastic core and the inner area of the fuel pellet could heal during normal operations. There is also no consideration given in this paper to the 'rim' region observed experimentally in the LWR fuel at extended burnup, despite the obvious barrier that the 'rim' will constitute to heat transfer.

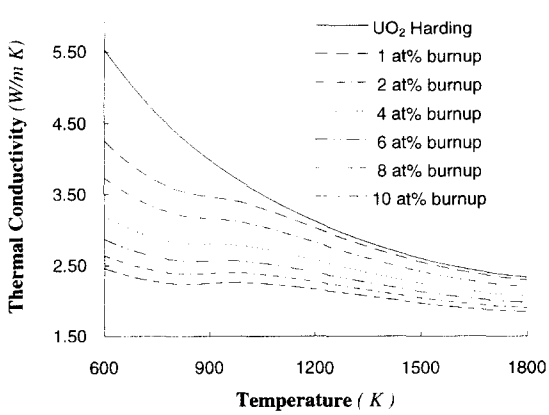

Fig. 9. Thermal conductivity of irradiated fuel for six different burnups (5 vol.% pore/bubble fraction) as a function of temperature as predicted by Eq. (14).

4. Validation based on irradiated fuel thermal conductivity data

There are five sources [6–8,10,11] from which the data on thermal conductivity of irradiated fuel are taken in this section. To validate the recommended expression for thermal conductivity of irradiated fuel, the available data will be briefly reviewed; the fit of the data and the inconsistencies encountered are also discussed.

One should also keep in mind that measurements of thermal conductivity of irradiated UO_2 fuel are subject to errors whether they are done in-pile or whether they are done out-of-pile. In-pile measurements usually give the thermal conductivity integral from centre-line temperature measurements and are affected by uncertainty in the gap conductance [59]. Out-of-pile measurements are done usually after some cooling time of the fuel (one or more years); after this time, radiation damage caused by decaying minor actinides (Pu-238, Am-241, Cm-242 and 244, etc.) grows in addition to the in-reactor damage. Furthermore, post-irradiation measurements are affected by precipitation of fission products and single gas atoms, microbubbles contained un the lattice at temperatures above 1100 K and by annealing of the radiation damage during measurements.

4.1. Chalk River data

In 1962, results from instrumented in-reactor experiments done at Chalk River Laboratories (CRL) were published [7]. The experiments concerned primarily measurements of fission-gas release from irradiated fuel. However, thermal conductivity was also deduced from the centre-temperature measurements of the irradiated fuel pellets.

The irradiated fuel thermal conductivity results were obtained over a large temperature range, from 500 to 2700 K and showed as well that the thermal conductivity of irradiated fuel is reduced compared with that of fresh UO_2. The Chalk River results are plotted in Fig. 10 along with the unirradiated UO_2 data and the prediction from Eq. (14). However, the burnup of these fuel pellets is small (a burnup of 0.9 at.% has been reported), so, the degradation occurred primarily because of radiation damage in the low temperature region. The CRL experimental data were lower than those from unirradiated UO_2 below 1400 K. The

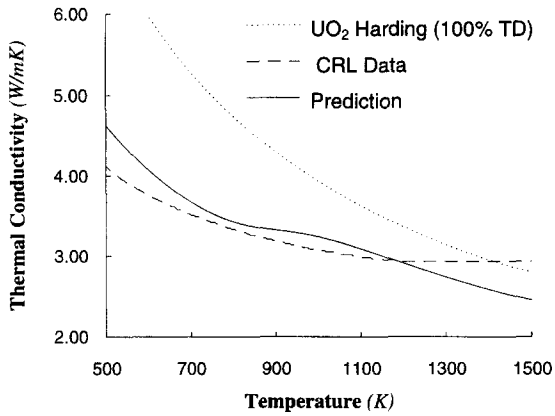

Fig. 10. Thermal conductivity results measured at Chalk River [7] on irradiated UO_2 compared to those of measured on fresh UO_2.

thermal conductivity values decrease with the temperature to about 1200 K and above they level and increase above 1500 K. Taking into account the large experimental errors in the measurements, a reasonable prediction of these results is obtained using the proposed analytical expression for the burnup of 0.9 at.% and a porosity of 7 vol.% (inital porosity of 6 vol.% was measured).

4.2. Bettis data

In 1964, Daniel and Cohen [6] reported in-pile measurements from Bettis Atomic Power Laboratories on irradiated fuel. They reported results from two experiments on fuel capsules containing hollow fuel pellets (BETT 69 series) and one containing solid pellets (WAPD series). The average values of effective thermal conductivity were obtained from three pairs of thermocouples in the WAPD 22-11 experiment (stainless steel capsule) and two pairs in the BETT 69-4 experiment (nickel capsule with alumina core). The data were obtained for centre temperatures up to 1050 K for solid pellets, and up to 900 K for the hollow pellets at various burnups to 10 at.%.

Despite the fact that the data are plotted and accurately tabulated, they are difficult to analyze. Their effective conductivity consists of two effects: fuel thermal conductivity and fuel-clad gap conductance. Most of the data span the temperature range for which the radiation damage has a significant impact. This fact could explain the relative large reduction in fuel thermal conductivity observed at low burnup (< 1 at.%).

However, their data show lower thermal conductivity for irradiated fuel and the degradation is higher as the burnup increases. The authors noticed a reduction in the effective thermal conductivity of UO_2 from 3.5 W/m K at 0.02 at.% burnup to 1.7 W/m K at 11 at.% burnup (28×10^{20} fission/cm^3). These values are not representative of constant operation since the fuel temperatures decreased significantly during irradiation. Nevertheless it was stated that the reduction was expected to be even larger at constant temperatures.

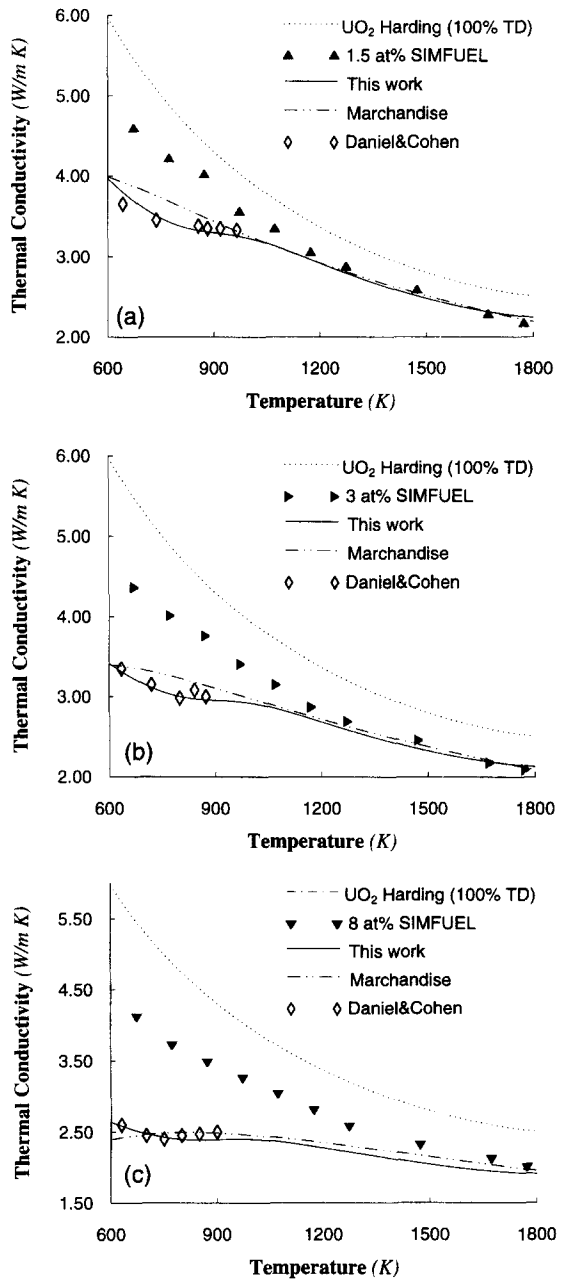

Fig. 11. (a) Irradiated fuel thermal conductivity (1.5 at.% burnup) as a function of temperature compared with Marchandise's expression [12] and irradiated fuel data from Daniel and Cohen [6]. The 1.5 at.% SIMFUEL [16] and UO_2 [3] data are also plotted. (b) The variation of irradiated fuel (3 at.% burnup) thermal conductivity compared with Marchandise's expression and irradiated fuel data from Daniel and Cohen. (c) The predicted thermal conductivity of irradiated fuel (8 at.% burnup) compared with Marchandise expression and irradiated fuel data from Daniel and Cohen.

The Bettis data reported by Daniel and Cohen [6] were carefully analyzed by Marchandise [12], who proposed an analytical expression as function of the burnup and temperature to fit Daniel and Cohen's data:

$$\lambda = \frac{1}{0.056 + 0.00021T + 18/T + b(6.184/T)} \quad (\mathrm{W/m\,K}), \tag{15}$$

where b is the burnup expressed as fission/cm^3 and T is the temperature in Kelvin. This expression was plotted by Marchandise for six different burnups between 0.2 and 3.2 at.%, and it was extrapolated to temperatures up to 1900 K. This expression and our Eq. (14) for the thermal conductivity of irradiated fuel are plotted comparatively in Fig. 11(a)–(c) for burnups of 1.5, 3 and 8 at.%, respectively. The unirradiated UO_2 and SIMFUEL (of equivalent burnup) data are also shown in the figures; Daniel and Cohen's measurements, corrected for gap conductance, are displayed for each burnup by open diamond symbols.

Clearly the measured SIMFUEL data for the same porosity represent the upper limit for the fuel thermal conductivity degradation, especially for temperatures below 1200 K where the effect of the precipitated fission products is negligible. Our proposed analytical expression for a porosity of 5 vol.% (reported for Bettis fuel [6]) and Marchandise's relation match well for each of the three burnups represented and both are in reasonable agreement with the experimental data of Daniel and Cohen corrected for the gap conductance. The small discrepancies with the experimental data could be easily attributed to the large experimental errors involved in the measurements of fuel central temperatures in-reactor.

4.3. High Burnup Chemistry Club data

More recent results on thermal conductivity of fuel irradiated for short times were obtained by the Belgonucleaire International High Burnup Chemistry Club (HBC) in the HBC-8 irradiation experiment [8]. The fuel, fabricated by Centre d'Etude Atomique (CEA), Cadarache had an initial enrichment of 7% U^{235} and high porosity, 7.3 vol.% consisting in 3.92 vol.% closed and 3.38 vol.% open porosity [60]. The shape of the pores was lenticular simulating interlinked bubbles formed at the grain boundaries. The fuel was irradiated in an instrumented assembly and the thermal conductivity of the fuel was deduced from the centerline temperature. These results were compared with Hyland's expression [2]. It was shown that an average of 35% reduction in thermal conductivity was obtained over the whole temperature range (from 800 to 1800 K); the results showed lower thermal conductivity and could be fitted by Hyland's formula multiplied by a factor of 0.65 especially for temperatures above 800 K, mainly to account for this special type of porosity.

We attempted to fit the data (Fig. 12) using Eq. (11b) for porosity and Eq. (14f) for the radiation damage factor.

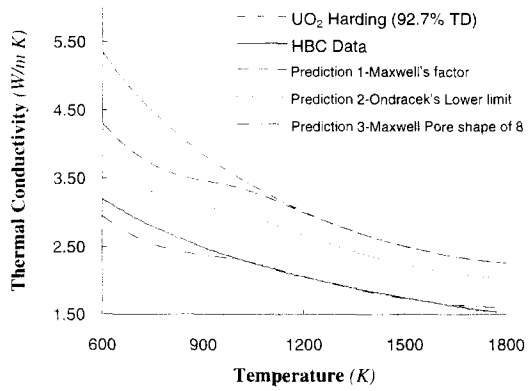

Fig. 12. Thermal conductivity of irradiated fuel from the HBC [8] irradiation experiment. These data were fitted by the radiation damage and the and the porosity factor applied to the UO_2 analytical expression.

However, the predicted values were higher than the measured values (prediction 1). Considering Eq. (11c), the prediction is still high in spite of using its lower limit $(1-p)^3$; this is shown by the dotted line (prediction 2) in Fig. 12. This result points out that the effect of pore and gas bubbles on irradiated fuel thermal conductivity is *not* adequately described by a porosity type factor, and use of a computational strategy [61] could improve the fit of the data.

In order to get a good fit of these experimental data, a large value of 8 for the pore shape factor, σ, and the average porosity value of 7.3 vol.% in Eq. (11) is required (prediction 3). The large pore shape factor is representative of the laminar pore morphology; similar effect of pore morphology on fuel thermal conductivity was found earlier in mixed oxide fuel [62]. These results point out once again that the pores/bubbles play a major role in a good prediction of irradiated fuel thermal conductivity and that the factors considered usually cannot describe properly the complex situation that occurs in irradiated fuel.

4.4. JAERI data

Recently, Nakamura et al. [10] reported thermal diffusivity results on irradiated fuel that reached relatively high burnup (of about 6.7 at.%). The irradiated fuel sample of irregular shape had been sliced from a fuel rod supplied by the Halden Project [63]. Additional measurements were performed on different specimens from the same rod. The new measurements confirmed the earlier results and span a larger temperature range (300 to 1600 K). The specimens are well characterized and the measured thermal diffusivity data were compared and found lower than those reported for SIMFUEL. Nakamura's latest thermal diffusivity measurements were converted to thermal conductivity using the specific heat of SIMFUEL and the density provided by the authors [64]. These values are plotted in Fig. 13(a) and (b).

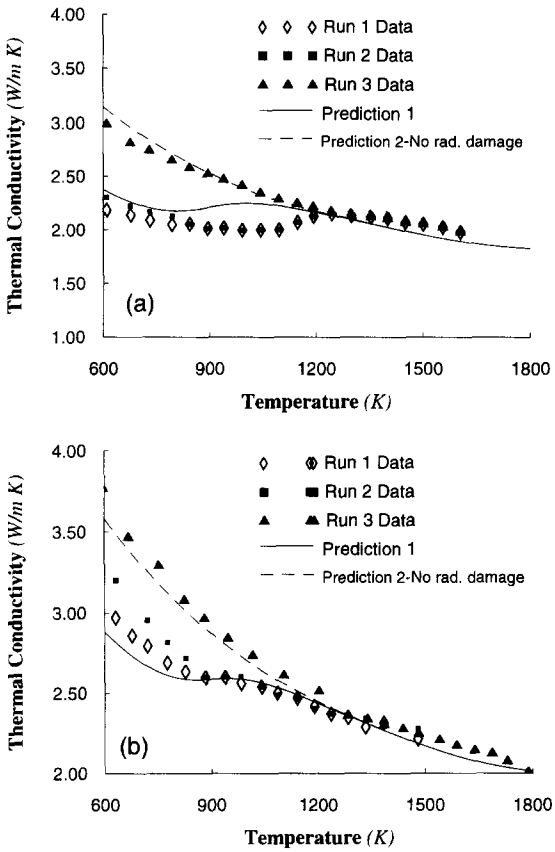

Fig. 13. (a) Thermal conductivity of irradiated fuel (sample 1 [64]) plotted by symbols and calculated values shown by continuous and broken line for the prediction with and without the radiation damage factor. (b) Thermal conductivity of irradiated fuel (sample 2 [64]) plotted by symbols and predicted values displayed by lines.

There were three consecutive thermal diffusivity measurements performed on each sample and the values were given as run 1, 2 and 3. The thermal diffusivity values in the low-temperature region below 1300 K, increased after each run because of recovery of the radiation damage defects [10]. Based on this observation the thermal conductivity expression has been used with and without the radiation damage factor κ_r to predict the measured values.

The thermal conductivities (deduced from thermal diffusivity measurements [64]) of two samples were quite different despite the fact they were obtained from the same fuel rod. Based on the microstructural characterization of the specimens, Nakamura found that there were differences in the microstructure of the two specimens. He estimated about 83–89% of theoretical density (TD) for the density of the first samples and about 92–96% TD for the second sample [63].

The predicted thermal conductivity of the first sample fits well the high-temperature region (Fig. 13(a)) of the experimental data when a porosity volume of 12 vol.% has been considered in the pore and bubbles factor. The prediction could not match well the lower experimental values at temperatures between 900 and 1200°C when single gas atoms and microbubbles annealing can play an important role [65]. Again, a good match is obtained for the second sample (scale 2 to 4 W/m K) for a pore/bubbles volume fraction of 4.8 vol.% in good agreement with the 4–8 vol.% estimated by Nakamura [64].

4.5. AEA Technology data

Thermal diffusivity measurements by the laser flash method on irradiated fuel samples from the Halden IFA 558 experiment have been recently reported by Carrol et al. [11]. The mean burnup of the fuel was 4.1 at.% (~ 40 GW d/t U). The authors reported results in the 600 to 1700 K temperature range on two irradiated samples for two heating and cooling runs on each sample. Unirradiated archive samples were also measured [11]. The thermal diffusivity values of irradiated fuel samples from the first heating cycle were depressed compared with the values of the unirradiated archive samples. The thermal diffusivity increased during the cooling cycle, especially for the lower temperature range. This hysteresis was explained by annealing of the radiation damage [11]. The authors also noticed a wide variation between the thermal diffusivity of unirradiated samples that persisted for the irradiated samples as well. They attributed this variability to the structure of the IFA 558 fuel, described as 'inhomogeneous' [11]. The density of the archive fuel was 10.439 g/cm^3 (95.25% of TD), and data are not available for the irradiated fuel [66].

The thermal diffusivity values were converted to thermal conductivity data using the density reported by the authors, corrected for temperature (the thermal expansion coefficient of the UO_2 was applied) and the appropriate specific heat values from SIMFUEL measurements. The thermal conductivity of the two samples are plotted as a function of the temperature in Fig. 14(a) and (b).

Using the pore and bubbles volume fraction from the density of the archive specimens and the shape factor for the spherical pores to calculate the thermal conductivity, we could not achieve a good fit from either one of the two samples (dotted lines in Fig. 14(a) and (b)). The predicted thermal conductivity that provided a good agreement for the first sample (Fig. 14(a)) was plotted using the reported burnup of the fuel [11] and a pore and bubble volume of 5 vol.% with a pore shape factor of 2.8. For the second sample, a good fit was obtained with the same pore and bubbles volume fraction of 5 vol.% and the pore/bubbles shape factor of 3.6. Both values of the pore and bubbles shape factor are higher than the standard value of 1.5 considered for spherical uniformly dispersed porosity. These pore shape factors reflect interlinked bubbles and tunnels formed in the fuel during irradiation as the IFA experiment was originally designated to investigate the possibility of delaying fission-gas bubble interlinkage by internal pressurisation. This internal pressurisation could

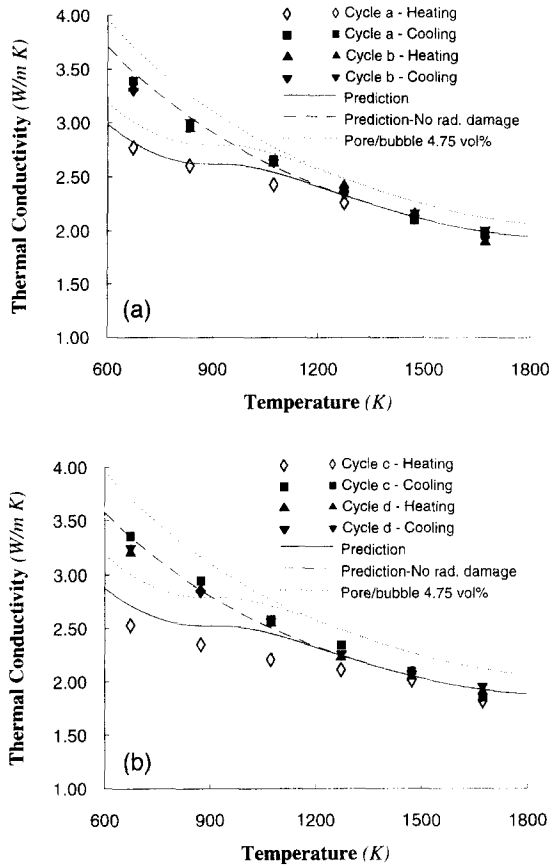

Fig. 14. (a) Thermal conductivity of irradiated fuel (sample 1 [11]) from IFA 558 experiment plotted by symbols and predicted values shown by lines. (b) Thermal conductivity of irradiated fuel (sample 2 [11]) plotted by symbols and calculated values shown by dotted and broken line for the prediction with and without the radiation damage factor.

also increase pore and bubble volume fraction to a level higher than normal. The interlinkage was reported to occur at a burnup of 24 MW d/kg U [11].

5. Conclusions

An analytical expression for thermal conductivity of irradiated UO_2 valid to 1900 K was derived by taking into account the effects of solid dissolved and precipitated fission products; porosity and fission-gas-bubbles, deviation from stoichiometry and radiation damage on intrinsic thermal conductivity of UO_2

- The effects of solid fission-product build-up and deviation from stoichiometry were assessed and quantified based on measured values and modelling of SIMFUEL results.
- The porosity factors were briefly reviewed (Loeb or Maxwell porosity factor), outlining the need for a better approach to quantify the pore/bubble factor based on experimental data.
- The radiation damage effect was quantified based on earlier measurements of irradiated fuel.

To validate the derived expression for the thermal conductivity of irradiated fuel UO_2 previous in-pile and thermal diffusivity experimental results were used:

- A reasonable agreement with the Chalk River data [7] was obtained.
- The results from Bettis [6], in the manner analyzed by Marchandise [12] were well fitted by the analytical function proposed for irradiated fuel.
- HBC data [8] on irradiated fuel with high porosity pointed out that the present approach to the pore and bubble effect is unsatisfactory.
- Recent thermal diffusivity data from JAERI [10] (converted to thermal conductivity) were well matched by the recommended expression for irradiated UO_2 fuel.
- Thermal diffusivity results from AEA [11] (translated into thermal conductivity) on irradiated fuel were well matched for the reported burnup and pore and bubble volume of 5 vol.% reported for archive fuel with a pore shape factor of 2.8 and 3.6 respectively.

Values of parameters (namely pore and bubble factor) could be chosen to provide a good fit to the experimental data. However, a means of selecting the pore and bubble shape factor and predicting the pore and bubble morphology and distribution as a function of burnup and temperature need to be determined.

Acknowledgements

The financial support for SIMFUEL work over the last five years from the CANDU Owners Group (COG) that made these results possible is acknowledged. Also, the authors thank many colleagues: M. Tayal, P.G. Boczar and D.S. Cox (AECL), F. Iglesias and E. Kohn (Ontario Hydro), P.G. Klemens (University of Connecticut), D. Olander (University of California at Berkeley), M. Lippens (Belgonucleaire), H. Kleykamp (KzK Karlsruhe), R.A. Gomme (AEA Windscale), W. Wiesenack (Halden), P. Chantoin (IAEA) and J. Nakamura (JAERI)) for their useful comments and suggestions on the manuscript. They would also like to express special thanks to M. Lippens (HBC), J. Nakamura (JAERI) and R.A. Gomme (AEA Windscale) for permission to use their results on irradiated fuel.

References

[1] D.G. Martin, J. Nucl. Mater. 110 (1982) 73.
[2] G.J. Hyland, J. Nucl. Mater. 113 (1983) 125.
[3] J.H. Harding and D.G. Martin, J. Nucl. Mater. 166 (1989) 166.
[4] A.B.G. Washington, UKAEA Report TRG 2236 (D) (1973).

[5] MATPRO-A Handbook of Materials Properties for Use in the Analysis of Light Water Reactor Fuel Rod Behaviour, TREE-NUREG-1005 (E.G. and G. Idaho, 1989).
[6] R.C. Daniel and I. Cohen, Bettis Atomic Power Report WAPD-246 (1964).
[7] J.A.L. Robertson, A.M. Ross, M.J.F. Notley and J.R. MacEwan, J. Nucl. Mater. 7 (1962) 223.
[8] S. Shibab, Belgonucleaire High Burnup Chemistry Club (HBC) Topical Report, HBC 91/34 (1991), private communication.
[9] W. Wiesenack, IAEA Tech. Comm. Meeting on Fission Gas Release and Fuel Rod Chemistry Related to Extended Burnup, 27 April–1 May 1992, Pembroke, Canada, IAEA-TECDOC-697, April (1993).
[10] J. Nakamura, H. Uetsuka, N. Kohno, E. Oheda, T. Sukegawa and T. Furuta, Enlarged Halden Programme Group Meeting, Bolkesjø, Norway, 30 October–4 November 1994, unpublished results.
[11] J.C. Carrol, R.A. Gomme and N.A. Leech, Enlarged Halden Programme Group Meeting, Bolkesjø, Norway, 30 October–4 November 1994, unpublished results.
[12] H. Marchandise, CEC Report EUR-4568f (1970).
[13] P.G. Lucuta, B.J. Palmer, Hj. Matzke and D.S. Hartwig, Proc. 2nd Int. Conf. on CANDU Fuel, ed. I.J. Hastings (CNS, Toronto, 1989) p. 132.
[14] P.G. Lucuta, R.A. Verrall, Hj. Matzke and B. Palmer, J. Nucl. Mater. 178 (1991) 48.
[15] Hj. Matzke, P.G. Lucuta and R.A. Verrall, J. Nucl. Mater. 185 (1991) 292.
[16] P.G. Lucuta, Hj. Matzke, R.A. Verrall and H.A. Tasman, J. Nucl. Mater. 188 (1992) 198.
[17] Hj. Matzke, P.G. Lucuta, R.A. Verrall and J.P. Hiernaut, in: 22nd Int. Conf. on Thermal Conductivity, 7–10 November 1993, Tempe, AZ, Proc. Thermal Conductivity 22, ed. T. Tong (Technomic, 1994) p. 904.
[18] P.G. Lucuta, R.A. Verrall, Hj. Matzke and I.J. Hastings, IAEA Tech. Comm. Meeting on Fission Gas Release and Fuel Rod Chemistry Related to Extended Burnup, 27 April–1 May 1992, Pembroke, Ont., Canada, IAEA-TECDOC-697, April (1993).
[19] P.G. Lucuta, R.A. Verrall, Hj. Matzke and I.J. Hastings, in: Proc. 3rd Int. Conf. on CANDU Fuel, ed. P.G. Boczar (CNS, Toronto, 1992) pp. 2–61.
[20] P.G. Lucuta, Hj. Matzke and R.A. Verrall, IAEA Tech. Comm. Meeting on Water Reactor Fuel Element Modelling at High Burnup and Experimental Support, Bowness-on-Windermere, UK, 18–23 September 1994.
[21] P.G. Lucuta, Hj. Matzke and R.A. Verrall, J. Nucl. Mater. 223 (1995) 51.
[22] P.G. Lucuta, Hj. Matzke and R.A. Verrall, J. Nucl. Mater. 217 (1994) 279.
[23] P.G. Lucuta, Hj. Matzke, R.A. Verrall and P.G. Klemens, in: 22nd Int. Conf. on Thermal Conductivity, 7–10 November 1993, Tempe, AZ, Proc. Thermal Conductivity 22, ed. T. Tong (Technomic, 1994) p. 894.
[24] P.G. Klemens and P.G. Lucuta, in: Proc. 23rd Thermal Conductivity Int. Conf., 30 Oct–1 Nov. 1995, Nashville, TN, to be published.
[25] R.W. Cahn, P. Haasen and Ej. Kramer, eds., Materials Science and Technology Handbook, Vol. 10a, Nuclear Materials, ed. B.R.T. Frost (VCH, 1994).
[26] J.A. Turnbull and M.O. Tucker, Philos. Mag. 30 (1974) 47.
[27] A.M. Ross, Atomic Energy of Canada Limited Report, AECL-1096 (1960).
[28] R.C. Hawkings and J.A.L. Robertson, Atomic Energy of Canada Limited Report, AECL-1733 (1963).
[29] R.C. Hawkings and A.S. Bain, Atomic Energy of Canada Limited Report, AECL-1790 (1963).
[30] E.H. Schmidt, J. Richter, Hj. Matzke and J. Van Geel, in: Proc. 22nd Int. Conf. on Thermal Conductivity, 7–10 November 1993, Tempe, AZ, Proc. Thermal Conductivity 22, ed. T. Tong (Technomic, 1994) p. 920.
[31] Summary sessions of IAEA Tech. Comm. Meeting on Water Reactor Fuel Element Modelling at High Burnup and Experimental Support, Bowness-on-Windermere, UK, 18–23 September 1994, IAEA Proc., to be published.
[32] G. Delette and M. Charles, IAEA Tech. Comm. Meeting on Water Reactor Fuel Element Modelling at High Burnup and Experimental Support, Bowness on Windermere, UK, 18–23 September 1994.
[33] H. Kleykamp, Report KfK 4170 (1970) 1245.
[34] J.A.L. Robertson, A.S. Bain and A. Ridal, Atomic Energy of Canada Limited Report, AECL-1037 (1960).
[35] S. Fukushima, T. Ohmichi, A. Maeda and H. Watanabe, J. Nucl. Mater. 105 (1982) 201.
[36] S. Fukushima, T. Ohmichi, A. Maeda and M. Handa, J. Nucl. Mater. 114 (1983) 312.
[37] F. Schmitz, G. Dean, M.Housseau, F. Keroulas and J.C. van Craeynest, in: Proc. Int. Meeting on Fast Reactor Fuel and Fuel Element, Karlsruhe, 1970, eds. M. Dalle Donne, K. Kummerer and K. Schroeder, p. 396.
[38] U. Runfors, ENEA Fuels and Mater. Spec. Meeting on Fast Gas-Cooled Breeders, Stockholm, 1969, Riso Report 269 (1972).
[39] V.I. Arimescu, private communications, AECL.
[40] Y. Philipponneau, J. Nucl. Mater. 188 (1992) 194.
[41] M. Beauvy, J. Nucl. Mater. 188 (1992) 232.
[42] I.R. Toplis, I.D. Palmer, S. Abeta, Y. Irisa and K. Yamate, IAEA Tech. Comm. Meeting on Recycling Plutonium and Uranium in Water Reactor Fuel, Newby Bridge, Windermere, UK, 3–7 July 1995.
[43] D. Baron and J.C. Couty, IAEA Tech. Comm. Meeting on Water Reactor Fuel Element Modelling at High Burnup and Experimental Support, Bowness-on-Windermere, UK, 18–23 September 1994.
[44] P.W. Winter and D.A. MacInnes, IAEA Tech. Comm. Meeting on Water Reactor Fuel Element Computer Modelling in Steady-State, Transient and Accident Conditions, Preston, UK, 1988.
[45] P.G. Klemens, High Temp. High Press. 23 (1991) 241.
[46] R.W. Rice, in: Treatise on Materials Science and Technology, Vol. 11, ed. R.K. MacCrone (Academic Press, New York, 1977) p. 199.
[47] Hj. Matzke, Science of Advanced LMFBR Fuels (North-Holland, Amsterdam, 1986) p. 176.
[48] D.P. White, J. Appl. Phys. 73 (1993) 2254.
[49] P. Nikolopoulos and G. Ondracek, J. Nucl. Mater. 114 (1983) 231.
[50] K. Bakker, H. Kwast and E.H.P. Cordfunke, J. Nucl. Mater. 223 (1995) 135.
[51] S.L. Hayes and K.L. Peddicord, J. Nucl. Mater. 202 (1993) 87.

[52] L.A. Goldsmith and J.A.M. Douglas, UKAEA Report TGR 2103(w) (1971).
[53] R.C. Hawkings and A.S. Bain, AECL Report AECL-1790 (1963).
[54] Hj. Matzke, J. Nucl. Mater. 223 (1995) 1.
[55] Hj. Matzke, J. Nucl. Mater. 208 (1994) 18.
[56] J.R. MacEwan and R.L. Stoute, J. Am. Ceram. Soc. 52 (1969) 160.
[57] M.E. Cunningam, M.D. Freshley and D.D. Lanning, J. Nucl. Mater. 188 (1992) 19.
[58] Hj. Matzke, J. Nucl. Mater. 189 (1992) 141; in: Ceramics Charting the Future, Advances in Science and Technology 3D, ed. P. Vincenzini (Techna Srl., 1995) p. 2913.
[59] W. Wiesenack, private communication.
[60] C. Forat and F. Guedeney, Report HBC 89/14 (1989), private communication.
[61] K. Bakker, H. Kwast and E.H.P. Cordfunke, J. Nucl. Mater. 226 (1995) 128.
[62] R.L. Gibby, Fabrication, Microstructure and Thermal Conductivity in UO_2–25 wt% PuO_2 Sintered Pellets, Report Handford Engineering Development Laboratory, HEDL-TME 72–88 (1972).
[63] W. Wiesenack, IAEA Tech. Comm. Meeting on Water Reactor Fuel Element Modelling at High Burnup and Experimental Support, Bowness-on-Windermere, UK, 18–23 September 1994.
[64] J. Nakamura, Fall Meeting of Atomic Energy Society of Japan, Tokai, 17–20 October 1995, private communication.
[65] J.A. Turnbull, 3rd IAEA Int. Coordination Meeting on Fuel Modelling at Extended Burnup, Bombay, India, 1–5 April 1996.
[66] R.A. Gomme, private communication.